Title
Activation of Tungsten Oxide for Propane Dehydrogenation and Its High Catalytic Activity and Selectivity

Journal
Catalysis Letters, 147(3)

ISSN
1011-372X

Authors
Yun, Yongju
Araujo, Joyce R
Melaet, Gerome
et al.

Publication Date
2017-03-01

DOI
10.1007/s10562-016-1915-2

Peer reviewed

Catal Lett
DOI 10.1007/s10562-016-1915-2

Activation of Tungsten Oxide for Propane Dehydrogenation and Its High Catalytic Activity and Selectivity

Yongju Yun[1,2] · Joyce R. Araujo[2,4] · Gerome Melaet[1,2] · Jayeon Baek[1,2] · Braulio S. Archanjo[2,4] · Myounghwan Oh[1,2] · A. Paul Alivisatos[1,2,3,5] · Gabor A. Somorjai[1,2,3,5]

Received: 31 August 2016 / Accepted: 8 November 2016

Abstract Dehydrogenation of propane to propene is one of the important reactions for the production of higher-value chemical intermediates. In the commercial processes, platinum- or chromium oxide-based catalysts have been used for catalytic propane dehydrogenation. Herein, we first report that bulk tungsten oxide can serve as the catalyst for propane dehydrogenation. Tungsten oxide is activated by hydrogen pretreatment and/or co-feeding of hydrogen. Its catalytic activity strongly depends on hydrogen pretreatment time and partial pressure of hydrogen in the feed gas. The activation of tungsten oxide by hydrogen is attributed to reduction of the metal oxide and presence of multivalent oxidation states. Comparison of the catalytic performance of partially reduced WO_{3-x} to other highly active metal oxides shows that WO_{3-x} exhibits superior catalytic activity and selectivity than Cr_2O_3 and Ga_2O_3. The findings of this work provide the possibility for activation of metal oxides for catalytic reactions and the opportunity for the development of new type of catalytic systems utilizing partially reduced metal oxides.

Graphical Abstract

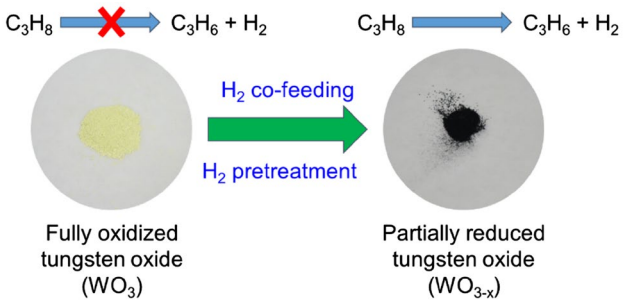

Keywords Heterogeneous catalysis · Dehydrogenation · Tungsten oxide · Reduction · Oxidation state

1 Introduction

Catalytic processes to produce value-added chemicals from light alkanes have attracted attention as a considerable amount of methane, ethane and propane is available from shale gas reservoirs in a cost-effective manner. The fact that propene, a product of dehydrogenation of propane, is used as feedstock for the production of valuable chemicals, including polymers, oxygenates and other chemical intermediates, motivates the study of propane dehydrogenation [1]. The increasing worldwide demand for propene also spurs the development of techniques to convert propane to propene exclusively rather than the utilization of

Electronic Supplementary Material The online version of this article (doi:10.1007/s10562-016-1915-2) contains supplementary material, which is available to authorized users.

✉ A. Paul Alivisatos
paul.alivisatos@berkeley.edu

✉ Gabor A. Somorjai
somorjai@berkeley.edu

[1] Department of Chemistry, University of California, Berkeley, CA 94720, USA

[2] Materials Sciences Division, Lawrence Berkeley National Laboratory, One Cyclotron Road, Berkeley, CA 94720, USA

[3] Chemical Sciences Division, Lawrence Berkeley National Laboratory, One Cyclotron Road, Berkeley, CA 94720, USA

[4] Materials Metrology Division, National Institute of Metrology, Quality and Technology, Duque de Caxias, RJ 25250-020, Brazil

[5] Kavli Energy NanoScience Institute, Berkeley, CA 94720, USA

Published online: 07 February 2017

conventional processes, yielding propene with low selectivity [2, 3]. Several catalytic dehydrogenation installations for the selective production of propene are under construction or planned [1].

Catalytic dehydrogenation of propane to propene ($C_3H_8 \leftrightarrow C_3H_6 + H_2$) is highly endothermic and thermodynamically limited reaction. Hence, it requires high reaction temperature above 550 °C to achieve propane conversion over 50% at atmospheric pressure [1, 4]. Noble metals and metal oxides exhibit catalytic activity and selectivity for C–H bond activation for propane dehydrogenation. However, severe deactivation of catalysts occurs by coke deposition on the surface of active materials and sintering of active phases of catalysts under the high temperature conditions [5–7]. In the case of dehydrogenation over metal oxides, the loss of activity and selectivity also arises from the oxidation state change of metal oxides during the reaction because both propane and hydrogen can act as reducing agents at the high temperatures [8, 9].

In spite of the fact that platinum- and chromium oxide-based catalysts show excellent catalytic performance and they are currently used in industrial processes, there have been attempts to develop new catalysts for propane dehydrogenation due to a high cost of the noble metal Pt and environmental toxicity of Cr^{6+} species [10]. It has been reported that in addition to CrO_x, various transition metal oxides, including GaO_x, VO_x, FeO_x, InO_x, ZrO_x and ZnO_x, are active for C–H bond activation of propane [1, 8, 11–20]. Previous study of propane dehydrogenation over ZrO_x promoted with La_2O_3 showed that the bulk metal oxide exhibits comparable catalytic activity to that of noble metal Pt [15]. Bulk Ga_2O_3 also showed a high propene selectivity of 95% while its activity was slightly lower than Cr_2O_3 for propane dehydrogenation at 500 °C [11]. These show that several metal oxides could be the promising catalysts for dehydrogenation of propane.

Recently, tungsten oxide is of great interest due to wide range of applications in heterogeneous catalysis, photochemistry, and electrochemistry [21–24]. The nonstoichiometry arising from oxygen vacancies and the presence of multivalent oxidation states often results in unique properties in catalysis [25, 26]. It has been shown that the bulk and supported tungsten oxides are catalytically active for dehydrogenation, hydrogenation and isomerization of hydrocarbons [25, 27, 28]. To the best of our knowledge, however, the catalytic properties of tungsten oxide for propane dehydrogenation have not been explored despite the fact that it is group VI transition metal oxide along with CrO_x, utilized as industrial catalysts. In this work, we report that bulk tungsten oxide is highly active and selective for propane dehydrogenation when it is partially reduced. Although fully oxidized bulk WO_3 is inactive under propane feed condition, co-feeding of H_2 and/or H_2 pretreatment activates the tungsten oxide. Its catalytic activity strongly depends on H_2 pretreatment conditions and H_2 partial pressure in the feed gas. The activation of tungsten oxide by H_2 is attributed to partial reduction of the metal oxide and the oxidation state change. The partially reduced tungsten oxide, WO_{3-x}, exhibits superior catalytic performance than those of Cr_2O_3 and Ga_2O_3, which are known as highly active metal oxides for propane dehydrogenation. The findings of this work open up the possibility for activation of several metal oxides by reduction and offer the opportunity for the development of new type of catalytic systems utilizing partially reduced metal oxides.

2 Experimental

2.1 Materials

Tungsten(VI) chloride (WCl_6, >99.9%), Pluronic P123 (M_n = ~5800, $EO_{20}PO_{70}EO_{20}$, EO = ethylene oxide, PO = propylene oxide), chromium(III) nitrate nonahydrate ($Cr(NO_3)_3{\cdot}9H_2O$, >99%) and gallium(III) nitrate hydrate ($Ga(NO_3)_3{\cdot}xH_2O$, >99%) were purchased from Sigma-Aldrich. All gases used in this study, propane, hydrogen, helium, nitrogen, argon (all ultra high purity, 99.999%) and air (extra dry), were supplied by Praxair.

2.2 Material Synthesis

Tungsten oxide was synthesized via the soft-templating method utilizing self-assembly of P123 [29]. For typical synthesis, 2 g of P123 was dissolved in 20 ml ethanol and stirred overnight at room temperature. A metal precursor solution was prepared separately by dissolving 4.0 g of tungsten (VI) chloride into 20 ml of ethanol. The tungsten precursor solution was slowly added to the solution containing P123 and stirred for 5 h. Then, the mixed solution was poured into Petri dishes and the solvent was slowly evaporated at 40 °C for 2 days and at 60 °C for another 2 days. The resulting sample was calcined in air at 400 °C for 6 h, followed by 700 °C for 6 h. For the comparison of catalytic performance, bulk Cr_2O_3 and Ga_2O_3 were prepared by thermal decomposition of $Cr(NO_3)_3{\cdot}9H_2O$ at 700 °C for 6 h in air and $Ga(NO_3)_3{\cdot}xH_2O$ at 750 °C for 3 h in air, respectively.

2.3 Material Characterization

Structural characterization of tungsten oxide was performed using a Philips CM200/FEG transmission electronic microscope (TEM) operated at 200 kV. The Brunauer–Emmett–Teller (BET) surface areas and pore volumes of metal oxides were measured via N_2 (ultra high

purity, 99.999%) physisorption at 77 K using Autosorb-1 (Quantachrome) analyzer. For temperature-programmed reduction (TPR), WO_3 sample of 200 mg was pretreated under Ar flow at 120 °C for 1 h. After the pretreatment, the catalyst was heated from 100 to 800 °C with a heating rate of 5 °C/min under a mixed gas flow (50 ml/min) of 10 vol% H_2 and 90 vol% Ar. The TPR profile was obtained by monitoring H_2 consumption using a thermal conductivity detector. X-ray diffraction (XRD) patterns were obtained by a Siemens D500 diffractometer using Cu Kα radiation source (1.54 Å). Chemical characterization of tungsten oxide was performed using a ultra-high vacuum (UHV) PHI 5400 X-ray photoelectron spectroscopy (XPS) system with a non-monochromatic Al X-ray source (Kα = 1486.7 eV) operated at 350 W power. Survey XPS spectra were obtained with analyzer pass energy of 178.5 eV and step size of 1 eV. High-resolution spectra of W 4 f were obtained with analyzer pass energy of 35 and 0.05 eV energy steps. There was no charging effect during the measurement of tungsten oxide samples. The peak fitting was performed using Casa XPS software. Binding energy values for the W $4f_{7/2}$ peak-shape were obtained from standard reference materials (commercial WO_3, WO_2 and metallic W from Sigma–Aldrich) and compared to the values analyzed under similar spectrometer conditions in literature [26, 30]. The metal peak was detected at 30.0 eV and has an asymmetric peak shape with a full-width at half maximum (FWHM) of 1 eV. The surface species of W^{6+}, W^{5+} and W^{4+} were fitted at 34.3 ± 0.2, 33.0 ± 0.2 and 31.3 ± 0.1 eV, respectively. An additional component corresponding to the W $5p_{3/2}$ peak was set at 7.5 eV above the W $4f_{7/2}$ peak from metallic W. The $W4f_{7/2}$–$4f_{5/2}$ doublet separation was 2.18 eV and peak area ratio was 4:3. Satellite peaks were set at 36.0 eV for metallic W and 40.0 eV for W^{6+} species, respectively.

2.4 Catalytic Measurements

The catalytic performance of tungsten oxide for propane dehydrogenation was evaluated in a tubular fixed-bed quartz reactor with 5 mm inner diameter. Typically, 200 mg of catalyst diluted with 400 mg quartz chips (total bed height 3.5 cm) was placed in the middle of the reactor and supported by a porous quartz frit inside the reactor. The catalyst was pelletized and sieved to yield 150–250 µm grain size before mixing with quartz chips of the same grain size.

In this study the total flow rate of feed gas was 50 ml/min and it was balanced with He. The flow rate of each gas was regulated using calibrated mass-flow controllers (Bronkhorst). The temperature was controlled using a type-K thermocouple positioned at the top of the catalytic bed inside of the quartz reactor and a PID controller. To avoid reaction of the thermocouple with feed gas, the thermocouple was shielded by quartz sheath. Prior to propane dehydrogenation reaction, the loaded catalyst was preheated to 650 °C with a heating rate of 10 °C/min for 85 min in a stream of He and then pretreated by H_2 (5 ml/min) or air (O_2, 5 ml/min) at 650 °C. After pretreatment, the reactor was cooled down to 600 °C while purging the reactor with He for 20 min. The propane dehydrogenation reaction was run with a flow of 4 ml/min of propane, corresponding to WHSV = 2.4 h^{-1}, under atmospheric pressure. A blank test showed that the conversion of propane at 600 °C by thermal cracking is <1%. In catalytic test conversion of propane ranged between 2 and 10%.

The reactant and products were analyzed using an online gas chromatograph (SRI GC 8610 C) equipped with a flame ionization detector (FID) and a thermal conductivity detector (TCD). All data were collected from 21 min with 6 min interval after steady-state is established. The propane conversion ($X_{C_3H_8}$), product selectivity (S_i) and surface area normalized activity were calculated as follows:

$$X_{C_3H_8}\,(\%) = \frac{n_{C_3H_8\ in} - n_{C_3H_8\ out}}{n_{C_3H_8\ in}} \times 100 \tag{1}$$

$$S_i(\%) = \frac{a_i}{3} \times \frac{n_i}{n_{C_3H_{8_{in}}} - n_{C_3H_{8_{out}}}} \times 100 \tag{2}$$

$$Activity\ (mol_{C_3H_8} m^{-2} s^{-1}) = \frac{F_{C_3H_8} \times X_{C_3H_8}}{SA} \tag{3}$$

where $n_{C_3H_8}$ is the number of moles of propane, n_i is the number of moles of C_1–C_3 products (CH_4, C_2H_4, C_2H_6 or C_3H_6), a_i is the number of carbon atoms in the corresponding product, $F_{C_3H_8}$ is the moles of propane fed per second, SA is BET surface area measured by N_2 adsorption, respectively. In the calculations, the conversion of propane to coke was not taken into account because the carbon balance was within ±3% deviation during the measurement.

3 Results

3.1 Characterizations of Fresh Samples

All samples for propane dehydrogenation were first prepared by calcining as-synthesized tungsten oxide in air at 400 °C for 6 h, followed by 700 °C for 6 h. The morphology, specific surface area, porosity, structure and oxidation state of the fresh samples were characterized by TEM, N_2 adsorption–desorption, XRD and XPS analysis. In this study a soft-templating approach utilizing the self-assembled supramolecular structure of organic surfactant was attempted to obtain a mesoporous structure with high surface area. However, the

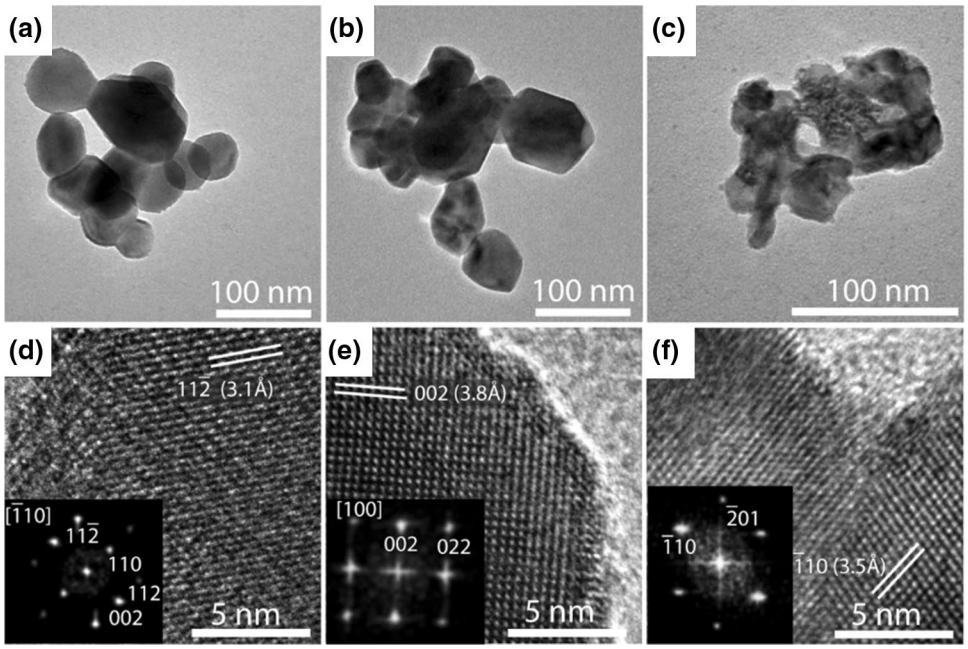

Fig. 1 TEM images and HR-TEM images (*inset* the corresponding FFT pattern) of tungsten oxide samples **a** and **d** before propane dehydrogenation reaction, **b** and **e** after reaction with C_3H_8, **c** and **f** after reaction with a gas mixture of C_3H_8 and H_2 ($H_2/C_3H_8 = 1$). The reaction with C_3H_8 in the absence of H_2 leads to no noticeable morphological changes. Co-feeding of C_3H_8 and H_2 results in aggregation of tungsten oxide particles. Reaction conditions: 0.2 g of catalyst, 50 ml/min of total flow rate, pretreatment with 50 vol% air at 650 °C for 1 h, propane dehydrogenation at 600 °C under atmospheric pressure for 12 h, $WHSV_{propane} = 2.4\ h^{-1}$

TEM image of the tungsten oxide sample calcined under air atmosphere shows no porous structure (Fig. 1a). The N_2 adsorption–desorption isotherm also exhibits the curves similar to those of nonporous materials (Fig. SI. 1). The low BET area of 6.3 m^2/g and pore volume of 0.082 cm^3/g of the sample confirm that utilizing the organic surfactant, P123, is not suitable for the preparation of mesoporous tungsten oxide for high-temperature reactions. The high-resolution (HR) TEM image of the prepared tungsten oxide shows interplanar distance of 3.1 Å, attributed to (11 $\bar{2}$) plane of WO_3 crystal structure (Fig. 1d). The corresponding fast Fourier transform (FFT) pattern is shown in the inset. The XRD diffractogram of the tungsten oxide sample in Fig. 2a reveals the diffraction peaks assigned to a monoclinic phase of WO_3 crystal (JCPDS Card No. 24–0747). The W 4f XPS spectra obtained from the WO_3 sample exhibit two sharp peaks at 34.3 eV (W $4f_{7/2}$) and 36.5 eV (W $4f_{5/2}$) and one broad satellite peak at 40.4 eV (Fig. 3a). These binding energies of W 4 f doublet peaks reveal that surface species of tungsten are in the state of W^{6+} [26]. This was also confirmed by comparing the W 4f XPS spectra of our sample with those obtained from commercial WO_3 sample (Sigma-Aldrich, Figure SI. 2), in which each peak exhibits nearly the same binding energies of 34.2 eV (W $4f_{7/2}$), 36.4 eV (W $4f_{5/2}$) and 40.5 eV (satellite WO_3 feature).

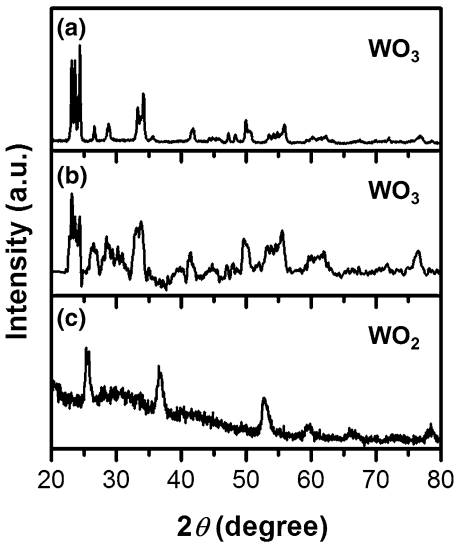

Fig. 2 XRD patterns of tungsten oxide samples **a** before propane dehydrogenation reaction **b** after reaction with C_3H_8 **c** after reaction with C_3H_8 and H_2 ($H_2/C_3H_8 = 1$). Following the reaction with C_3H_8, the spent catalyst shows the similar XRD pattern to the fresh WO_3 catalyst. Co-feeding of H_2 and C_3H_8 leads to the structural change from WO_3 to WO_2. Reaction conditions: 0.2 g of catalyst, 50 ml/min of total flow rate, pretreatment with 50 vol% air at 650 °C for 1 h, propane dehydrogenation at 600 °C under atmospheric pressure for 12 h, $WHSV_{propane} = 2.4\ h^{-1}$

3.2 Catalytic Performance for Propane Dehydrogenation

3.2.1 Activation of Tungsten Oxide by Co-feeding of H_2

The catalytic performance of the prepared WO_3 samples for propane dehydrogenation was studied at 600 °C with increasing H_2/C_3H_8 ratio in feed gas; $H_2/C_3H_8 = 0$, 0.5, 1 and 2. Before the reaction, the WO_3 samples were pretreated at 650 °C for 1 h under air flow as described above. Figure 4a, b show specific activity normalized by BET surface area of the sample and selectivity towards C_3H_6,

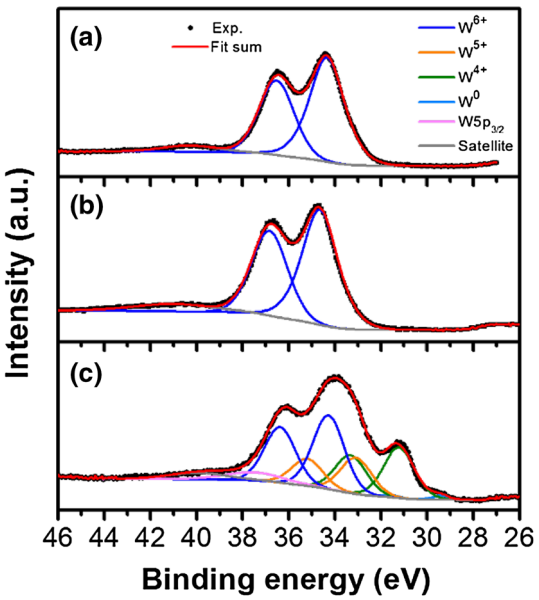

Fig. 3 Fitted W 4f XPS spectra of tungsten oxide samples **a** before propane dehydrogenation reaction **b** after reaction with C_3H_8 **c** after reaction with C_3H_8 and H_2 ($H_2/C_3H_8=1$). When a fresh WO_3 sample is reacted with C_3H_8 without H_2, there is no change in the oxidation state, showing W^{6+}. Co-feeding of H_2 and C_3H_8 results in partial reduction of the sample during the reaction, exhibiting W^{6+}, W^{5+}, W^{4+} and W^0. Reaction conditions: 0.2 g of catalyst, 50 ml/min of total flow rate, pretreatment with 50 vol% air at 650 °C for 1 h, propane dehydrogenation at 600 °C under atmospheric pressure for 12 h, $WHSV_{propane} = 2.4\ h^{-1}$

respectively. When propane is only present in the feed gas, the WO_3 catalyst exhibits negligible activity and low C_3H_6 selectivity arising from thermal cracking of propane. Co-feeding of H_2 and propane, however, results in a remarkable increase of activity and selectivity during the initial period of reaction, activating the catalyst. The increase of H_2/C_3H_8 ratio in the feed gas from 0.5 to 1 to 2 leads to higher activity although it results in rapid activation and deactivation of the catalyst. At the feed ratios of $H_2/C_3H_8=0.5$ and 1, the C_3H_6 selectivity of the activated tungsten oxide is quite stable, showing ~90% selectivity. However, an excess of H_2 in the feed ($H_2/C_3H_8=2$) leads to a lower C_3H_6 selectivity of ~84% and it decreases further after a time of the stream of ~300 min. The decrease of selectivity is mainly attributed to the increase of methane (CH_4) production.

In order to elucidate the influence of co-feeding of H_2 on the activation of the catalysts for propane dehydrogenation, the morphology, bulk structure and the oxidation state of spent samples were analyzed by TEM, XRD and XPS. After 12 h reaction with propane in the absence of H_2 ($H_2/C_3H_8=0$) at 600 °C, no noticeable morphological changes were observed in TEM images (Fig. 1b). The spent catalyst shows the similar XRD pattern to that of the fresh sample before the reaction (Fig. 2b). The fact that spent sample has a lattice spacing of 3.8 Å corresponding to (002) interplanar distance of WO_3 supports the XRD results (Fig. 1e). The binding energies of W 4f and the atomic ratio of $O/W \approx 3$ measured from the spent catalyst indicate the existence of only W^{6+} species on the surface (Fig. 3b). This is confirmed by the observation that the spent catalyst showed the same pale-yellow color as the fresh sample. These results clearly demonstrate that the fully oxidized WO_3 undergoes no structural and chemical changes under propane flow at 600 °C and the WO_3 sample is inactive for propane dehydrogenation.

However, the catalyst reacted with the feed gas mixture of C_3H_8 and H_2 ($H_2/C_3H_8=1$) shows agglomeration of tungsten oxide particles (Fig. 1c). The HR-TEM image exhibits the interplanar distances of 3.5 Å, corresponding

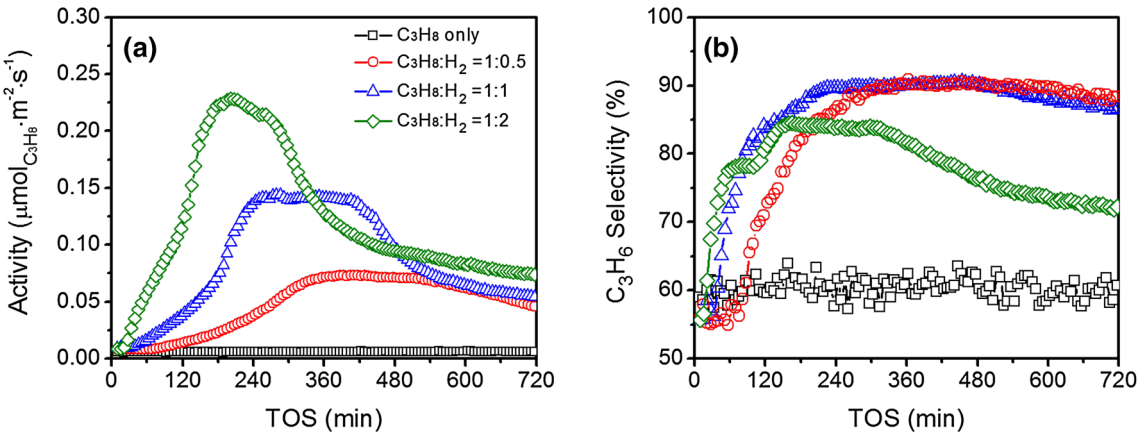

Fig. 4 **a** Specific activity and **b** C_3H_6 selectivity as a function of time of stream under different feed conditions (C_3H_8 only, $H_2/C_3H_8=0.5$, 1 and 2). Tungsten oxide exhibits negligible activity and low selectivity when it is reacted with C_3H_8. The catalyst is activated by co-feeding of H_2 and C_3H_8. Reaction conditions: 0.2 g of catalyst, 50 ml/min of total flow rate, pretreatment with 50 vol% air at 650 °C for 1 h, propane dehydrogenation at 600 °C under atmospheric pressure for 12 h, $WHSV_{propane} = 2.4\ h^{-1}$

to the ($\bar{1}10$) plane of WO_2 (Fig. 1f). As shown in Fig. 2c, the structural change from WO_3 to WO_2 during the reaction is also observed in the XRD diffractogram, where the peaks at $2\theta = 25.8°$, 36.6° and 52.8° are assigned to monoclinic WO_2 phase (JCPDS Card No. 05-0431). Moreover, the W 4f XPS spectrum of the spent catalyst clearly reveals new peaks at lower binding energies (Fig. 3c). This shows that W^{6+} species on the surface of the WO_3 sample were reduced to W^{5+}, W^{4+} and W^0, corresponding to 33.1, 31.3 and 30.0 eV for W $4f_{7/2}$, respectively. As a consequence of this partial reduction under the flow of gas mixture with $H_2/C_3H_8 = 1$, the surface atomic O/W ratio of the spent catalyst decreased from 3 to 2.42. It is noteworthy that no peaks corresponding to WO_3 phase were visible in the XRD patterns whereas a considerable amount of W^{6+} species was observed in XPS spectrum. This discrepancy arises from re-oxidation of the partially reduced tungsten oxide surface by air exposure while preparing sample for XPS analysis [27]. It should also be noted that the color of the sample was changed from pale yellow to deep blue after the propane dehydrogenation reaction. These observations clearly indicate that the activation of tungsten oxide during the propane dehydrogenation as shown in Fig. 4 is attributed to the reduction of the catalyst by the gas mixtures of H_2 and C_3H_8.

3.2.2 *Activation of Tungsten Oxide by H_2 Pretreatment*

The influence of reduction on the catalytic performance of tungsten oxide for propane dehydrogenation was further studied by varying pretreatment conditions. TPR profile showed that a fresh WO_3 sample starts to be reduced at ~650 °C by H_2 (Fig. SI. 3). For a comparison of catalytic properties of fully oxidized WO_3 and reduced sample, fresh WO_3 catalysts were pretreated under the flow of H_2 or air for 1h at 650 °C and then, purged by He while cooling down the reactor to a reaction temperature of 600 °C. Figure 5a, b show specific activity and C_3H_6 selectivity of the pretreated tungsten oxides under the flow of a gas mixture with $H_2/C_3H_8 = 1$. For air-pretreated catalyst, an induction period (~50 min)

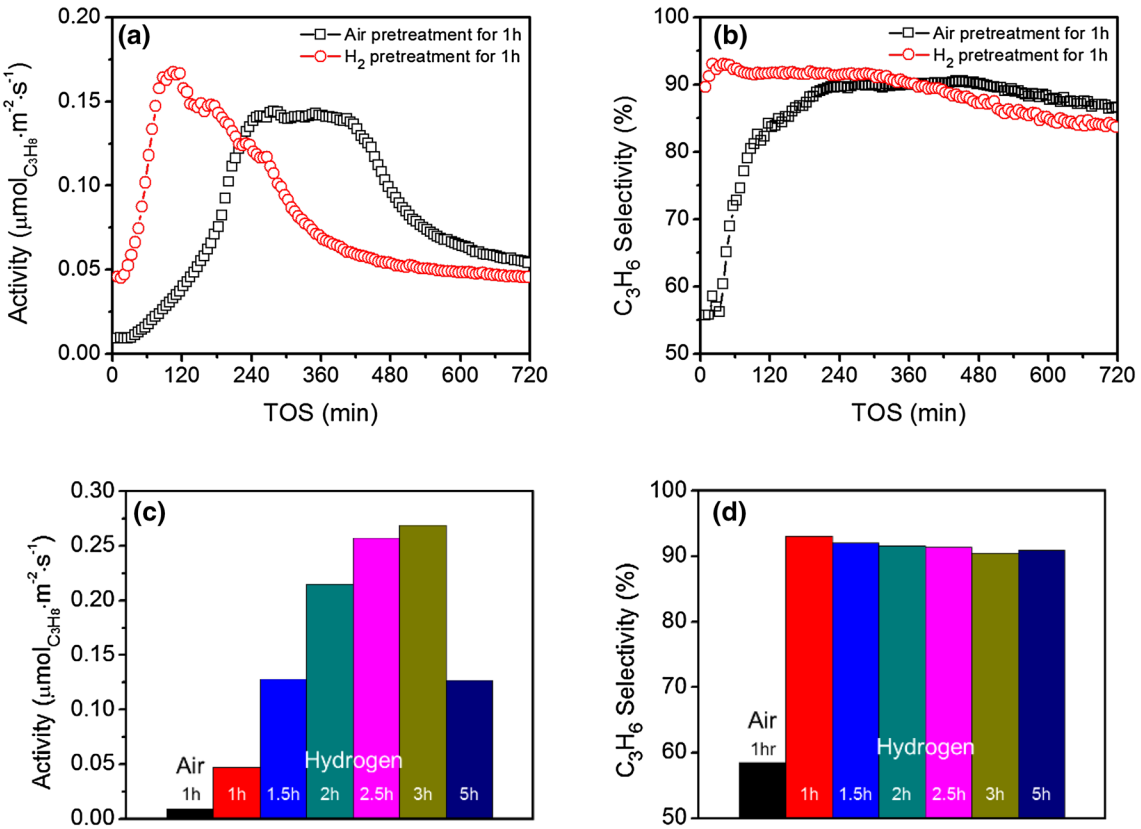

Fig. 5 **a** Specific activity and **b** C_3H_6 selectivity as a function of time of stream under different pretreatment conditions (air or H_2 pretreatment for 1 h) **c** initial specific activity and **d** initial C_3H_6 selectivity at TOS = 21 min under different pretreatment conditions. Tungsten oxide is activated by H_2 pretreatment and the initial activity strongly depends on the duration of H_2 pretreatment. Reaction conditions: 0.2 g of catalyst, 50 ml/min of total flow rate, pretreatment with 50 vol% of air or 10 vol% of H_2 at 650 °C, propane dehydrogenation with C_3H_8 and H_2 at 600 °C under atmospheric pressure, $H_2/C_3H_8 = 1$, $WHSV_{propane} = 2.4\ h^{-1}$

is required to exhibit catalytic activity. However, the formation of propene and high selectivity of ~90% are readily observable after H_2 pretreatment. Under the flow of the gas mixture of C_3H_8 and H_2, the H_2-pretreated catalyst is further activated up to 105 min and then starts to be deactivated. These imply that partially reduced tungsten oxide, WO_{3-x}, shows higher activity and selectivity than fully oxidized WO_3 and the catalytic performance depends on the degree of reduction of tungsten oxide. The effect of reduction on the intrinsic catalytic performance of tungsten oxide was also investigated by varying the duration of H_2 pretreatment (Fig. 5c, d and Figure SI. 4). The results show that the initial activity of the tungsten oxide noticeably increases up to 3 h pretreatment and then decreases after a longer pretreatment of 5 h. However, all catalysts exhibit similar C_3H_6 selectivity between 90 and 93%, showing that the initial selectivity is not affected by the H_2 pretreatment time (Fig. 5d).

To understand the influences of H_2 pretreatment, the TEM, XRD and XPS results obtained from 2.5 to 5 h H_2-pretreated tungsten oxide samples were compared to fresh WO_3 sample. Both H_2-pretreated samples exhibit severe aggregation of tungsten oxide particles (Fig. 6a, b). The XRD patterns demonstrate that they are reduced during the H_2 pretreatment (Fig. 6c, d). The sample pretreated by H_2 for 2.5 h exhibits apparent peaks assigned to monoclinic WO_2 phase (JCPDS Card No. 05-0431) and small peaks corresponding to the crystalline cubic phase of metallic W (JCPDS Card No. 04-0806). The formation of the metallic W phase is clearly evidenced for the sample pretreated for 5 h. This observation shows that WO_3 is reduced further by longer H_2 pretreatment time. The W 4f XPS spectra for the H_2-pretreated samples reveal the oxidation state change from W^{6+} to multiple oxidation states including W^{6+} (34.2 eV), W^{5+} (33.0 eV), W^{4+} (31.2 eV) and W^0 (29.6 eV) (Fig. 6e, f). Therefore, the high activity of the tungsten oxide catalyst pretreated by H_2 for 2.5 h results from the partial reduction of tungsten oxide and its multivalent oxidation states. A clear difference between the tungsten oxide catalysts reduced for 2.5 and 5 h is the atomic compositions of surface W^0 species. Although the composition of W^0 species is 8% for the sample pretreated for 2.5 h, it increases up to 26% after 5 h H_2 reduction (Table 1). The existence of metallic W is observed in the HR-TEM image, in which the sample has a lattice spacing (2.3 Å) corresponding to (110) plane of the cubic metallic W (inset in Fig. 6b). Considering a drop of catalytic activity after 5 h H_2 pretreatment in Fig. 5c, a negative effect by the over-reduction is attributed to the formation of metallic tungsten phases on the surface.

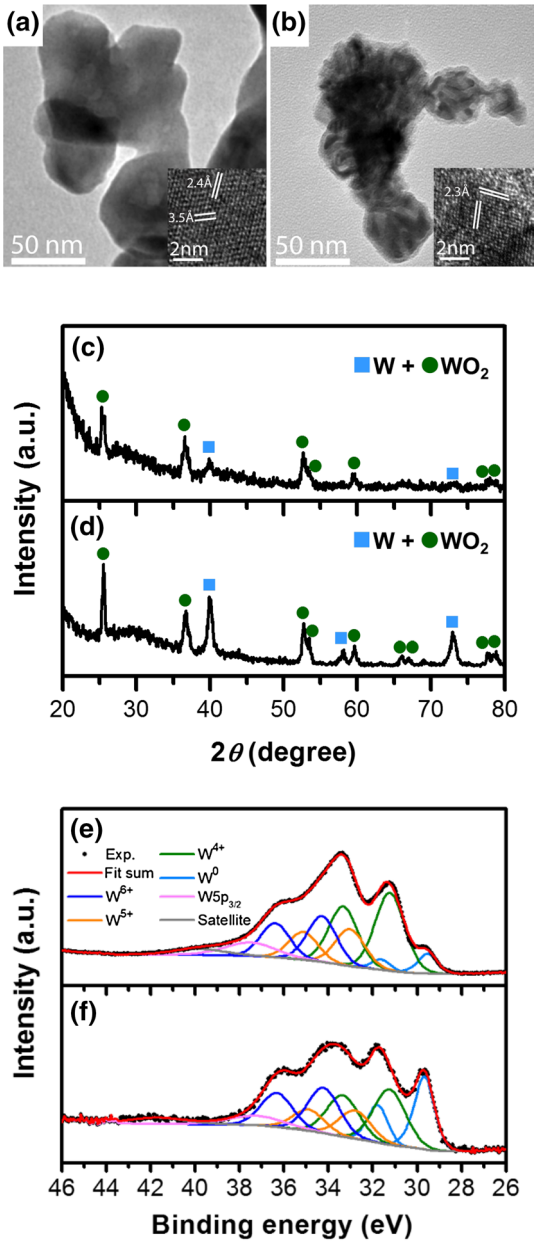

Fig. 6 TEM images (*inset* high-resolution TEM images) of tungsten oxide samples pretreated with H_2 for **a** 2.5 h and **b** 5 h. XRD patterns tungsten oxide samples pretreated with H_2 for **c** 2.5 h and **d** 5 h. Fitted W 4f XPS spectra of tungsten oxide samples pretreated with H_2 for **e** 2.5 h and **f** 5 h. These show that a fresh WO_3 sample is partially reduced by H_2 pretreatment, exhibiting multiple oxidation state of W^{6+}, W^{5+}, W^{4+} and W^0. Longer pretreatment time leads to a higher concentration of metallic W. Reaction conditions: 0.2 g of catalyst, 50 ml/min of total flow rate, pretreatment with 10 vol% H_2 at 650 °C

3.2.3 *Catalytic Performance of Partially Reduced Tungsten Oxide*

For the evaluation of the catalytic performance, the catalytic activity and the selectivity of partially reduced

Table 1 Surface composition of W species measured by XPS analysis

Catalyst	W^{6+} (%)	W^{5+} (%)	W^{4+} (%)	Metallic W (%)
Fresh sample	100	0	0	0
2.5 h H_2-pretreated sample	26	21	45	8
5 h H_2-pretreated sample	26	16	32	26

tungsten oxide, WO_{3-x}, were compared to those of other highly active bulk metal oxides such as Cr_2O_3 and Ga_2O_3 (Fig. 7a, b and Figure SI. 5a, b). The catalytic tests for all metal oxides were conducted at 600 °C under the feed of C_3H_8 in the absence of H_2. As shown in Fig. 5, pretreatment conditions affect the catalytic performance of metal oxides. Therefore, the samples of WO_3 and Cr_2O_3 were pretreated in air or H_2 before propane dehydrogenation to find out optimal pretreatment conditions for each metal oxide. In the case of Ga_2O_3, it was only pretreated in air because reduction of the metal oxide by H_2 can lead to the formation of volatile or liquid phases under the reaction condition. As expected, partially reduced WO_{3-x} showed higher activity and selectivity than fully oxidized WO_3. In contrast, Cr_2O_3 exhibited better catalytic performance when it was air-pretreated. It is noteworthy that higher activity of air-pretreated Cr_2O_3 is attributed to the fact that Cr^{6+} species plays a role as the precursor to produce the most active surface species [9]. The easy reducibility of Cr_2O_3 and therefore, the total loss of Cr^{6+} species by H_2 pretreatment appears to result in lower activity. The comparison of the catalytic performance of three metal oxides after the optimal pretreatment is shown in Fig. 7a, b. The partially reduced WO_{3-x}, obtained by 2.5 h H_2 pretreatment, has more than three times higher initial activity than air-pretreated Cr_2O_3 and Ga_2O_3. The WO_{3-x} sample also exhibits superior C_3H_6 selectivity of ~96% than other metal oxides for the propane dehydrogenation at 600 °C. A rapid deactivation of metal oxide catalysts during propane dehydrogenation requires frequent regeneration of the catalysts. In the commercial Catofin process, CrO_x/Al_2O_3 catalyst is typically regenerated after 12 min of dehydrogenation at 575 °C. Although the partially reduced WO_{3-x} catalyst shows high activity and selectivity during the reaction at 600 °C, fast deactivation is still observed as shown in Figure SI. 5a.

The influence of pre-reduction on the activity and selectivity was further studied by repeating propane dehydrogenation for 1 h (Fig. 8a, b). The fresh WO_3 sample was pre-reduced at 650 °C for 2.5 h for the 1st cycle of reaction. After the propane dehydrogenation reaction, the catalyst was regenerated under air flow at 650 °C for 20 min, followed by over-reduced with H_2 for 3.5 h on purpose. During several reaction cycles (2nd–12th cycles), the initial activity and the selectivity of WO_{3-x} gradually decrease, exhibiting deactivation. However, shorter pretreatment, 3 h H_2 pretreatment, results in better the catalytic performance as shown for the 13th–16th cycles. Although a further shorter pre-reduction for 2.5 h leads to the lower activity and the selectivity as measured in the 17th cycle, the catalytic efficiency is recovered to the pervious values after 3 h pretreatment. This suggests that there is an optimal chemical state to obtain the best catalytic performance and it can be achieved by controlling the H_2 pretreatment time. It is also noteworthy that despite its deactivation during the repeated cycles, the

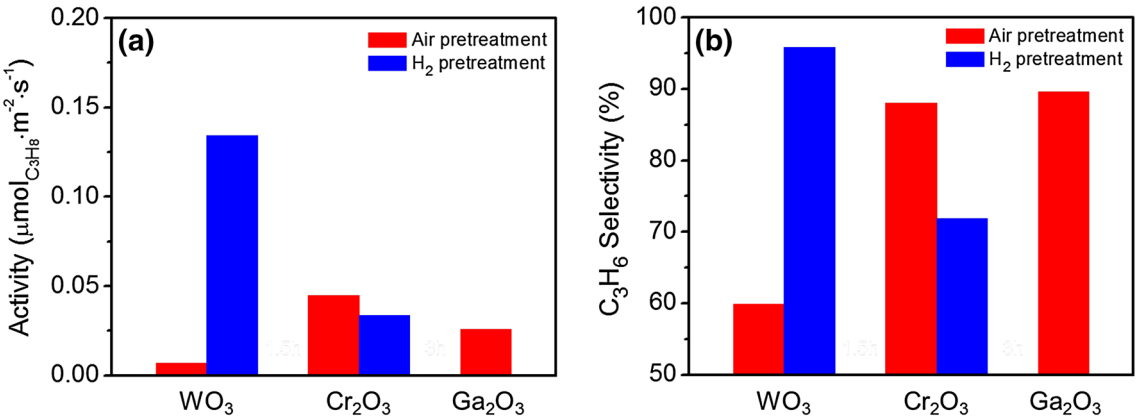

Fig. 7 **a** Initial specific activity and **b** C_3H_6 selectivity of air or H_2-pretreated WO_3, Cr_2O_3 and Ga_2O_3 at TOS = 21 min. The partially reduced tungsten oxide shows superior catalytic activity and selectivity than other highly active metal oxides, Cr_2O_3 and Ga_2O_3. Reaction conditions: 0.2 g of catalyst, 50 ml/min of total flow rate, pretreatment with 10 vol% H_2 for WO_3 (2.5 h) and Cr_2O_3 (1 h) or pretreatment with 50 vol% air for WO_3 (1 h), Cr_2O_3 (1 h) and Ga_2O_3 (1 h) at 650 °C, propane dehydrogenation with only C_3H_8 at 600 °C under atmospheric pressure, $WHSV_{propane} = 2.4\ h^{-1}$

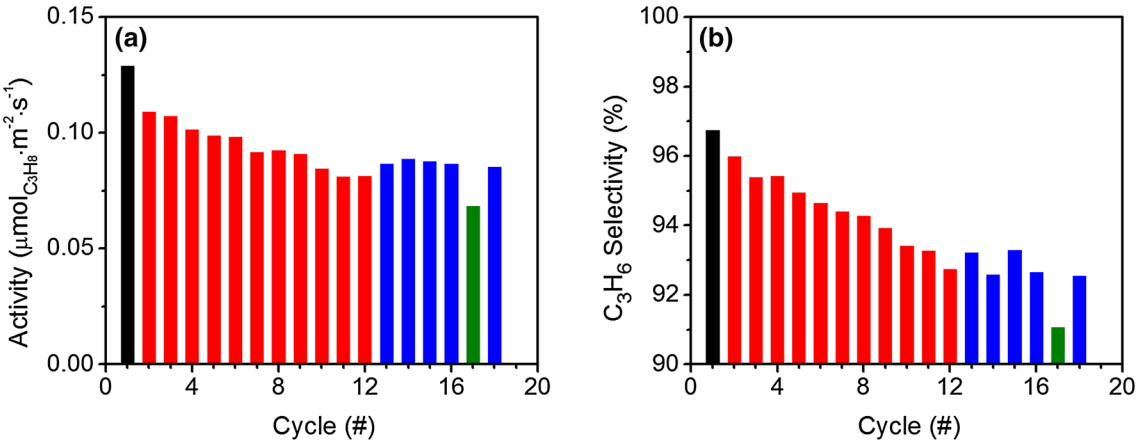

Fig. 8 **a** Initial specific activity and **b** initial C_3H_6 selectivity at TOS = 21 min over 18 H_2 pretreatment—propane dehydrogenation—air regeneration cycles. Initially tungsten oxide sample was pretreated with 10 vol% H_2 at 650 °C for 2.5 h (*black*). After the 1st reaction, the regenerated sample was pretreated with H_2 at 650 °C for 3.5 h (*red*), 3 h (*blue*) and 2.5 h (*green*), respectively. Varying H_2 pretreatment duration and therefore, controlling the oxidation state of tungsten oxide affects catalytic activity and selectivity. Reaction conditions: 0.2 g of catalyst, 50 ml/min of total flow rate, propane dehydrogenation with only C_3H_8 at 600 °C under atmospheric pressure, $WHSV_{propane}$ = 2.4 h^{-1}, regeneration with 50 vol% air at 650 °C for 20 min

activity and selectivity of WO_{3-x} catalyst at 18 cycle are still higher than those of fresh Cr_2O_3 and Ga_2O_3 catalysts.

4 Discussion

A key observation of this work is that the reduction of bulk WO_3 by co-feeding of H_2 and/or H_2 pretreatment activates the tungsten oxide catalyst for propane dehydrogenation although fully oxidized WO_3 is inactive. Moreover, the partially reduced WO_{3-x} shows superior catalytic performance than bulk Cr_2O_3 and Ga_2O_3, reported as highly active catalysts for propane dehydrogenation. These observations raise fundamental questions about the characteristics of WO_{3-x} governing its catalytic activity and the specific active sites for propane dehydrogenation. A directly observable change arising from reduction by H_2 in the pretreatment step or during the reaction with gas mixtures of C_3H_8 and H_2 is a variation of the oxidation state of the tungsten oxide catalysts. The influence of oxidation state on alkane dehydrogenation over metal oxides has been extensively studied for chromium oxide [9, 31–33]. It has been suggested that Cr^{3+} cation is the most active for dehydrogenation reactions among Cr^{6+}, Cr^{5+}, Cr^{3+} and Cr^{2+} surface species [33, 34]. Also, a close relationship between oxidation state of metal ion and activity has been observed in dehydrogenation over supported VO_x, in which V^{3+} ion showed higher active than V^{5+} and V^{4+} species [20]. Indeed, our results obtained from catalytic measurement and XPS analysis confirm that the activity and selectivity of tungsten oxide are influenced by its oxidation state. Although the presence of only W^{6+} species on the surface of tungsten oxide leads to no activity and poor selectivity, the evolution of multivalent oxidation state results in high catalytic performance for propane dehydrogenation. In repeated cycles the variation of oxidation state of WO_{3-x} also determines its catalytic efficiency as shown in Fig. 8. Therefore, we expect that oxidation state of tungsten oxide is a factor governing its catalytic activity for propane dehydrogenation.

The complexity arising from the presence of multivalent W cations on the surface hampers the identification of specific active sites of partially reduced WO_{3-x} for propane dehydrogenation. However, similar activation of tungsten oxides by H_2 reduction has been reported for isomerization reactions, which involve dehydrogenation as the first reaction step [27, 35]. It was suggested that dehydrogenative properties of WO_{3-x} are attributed to W^{4+} cations with free electrons [27]. Our XPS result for the highly active tungsten oxide, pretreated for 2.5 h, also shows that W^{4+} species has the highest concentration of 45% among the surface W species (Table 1). Therefore, we suggest that W^{4+} species is the most likely active site for the propane dehydrogenation. However, the possibility cannot be ruled out that other W cations or the interfaces between various W species are active for propane dehydrogenation. Recently, it was observed that slightly reduced WO_{3-x} with W^{6+} and W^{5+} cations exhibits improved catalytic activity compared to fully oxidized WO_3 with only W^{6+} cation for hydrogenation of cyclohexane [25]. This implies that the catalytic properties, responsible for hydrogenation and dehydrogenation, also arise from W^{5+} species or the interface between W^{6+} and W^{5+} cations. The presence of a considerable amount of metallic tungsten species has a negative effect on the

activity for propane dehydrogenation as shown for 5 h pretreated sample in Fig. 5c. However, it should be noted that W^0 species can often contribute to dehydrogenation of saturated hydrocarbon [36]. It was shown that the reduced WO_{3-x} with W^{6+}, W^{5+}, W^{4+} and a small amount of W^0 species reveals higher conversion and selectivity towards dehydrogenation reaction than those with only W^{6+}, W^{5+} and W^{4+} cations [27]. Indeed, the tungsten oxide pretreated by H_2 for 2.5 h exhibits excellent catalytic performance for propane dehydrogenation although it includes 8% of W^0 species. This implies that the metal-oxide interfaces between metallic tungsten and tungsten oxides may play an important role in the dehydrogenation of propane.

The nature of active sites, oxidation state and the catalytic properties of tungsten oxide mentioned above are closely inter-correlated. Therefore, further careful experiments are needed for deep understanding of the superior activity of partially reduced WO_{3-x} for propane dehydrogenation. It is also interesting to see whether the modification of catalytic characteristics by control of oxidation state can be applied to other metal oxides. We are conducting experiments to understand the influence of those properties and exploring the control of the catalytic performance to propane dehydrogenation by using oxidizing and reducing agents.

5 Conclusions

Fully oxidized bulk tungsten oxide, WO_3, is inactive for propane dehydrogenation. However, tungsten oxide can be activated by H_2 pretreatment and/or co-feeding of H_2 during the reaction. The reduction and oxidation state change of the tungsten oxide in the H_2 environment were confirmed by HR-TEM, XRD and XPS. The catalytic activity of the WO_{3-x} catalysts strongly depends on the H_2 reduction conditions. After the H_2 pretreatment, the partially reduced WO_{3-x} shows superior catalytic activity and selectivity than those of other highly active metal oxides, Cr_2O_3 and Ga_2O_3.

Acknowledgements We thank the financial support from the Dow Chemical Company through funding for the Core–Shell Catalysis Project, Contract No. 20120984 to University of California, Berkeley. The user project at the Molecular Foundry was supported by the Office of Science, Office of Basic Energy Sciences, of the U.S. Department of Energy under Contract No. DE-AC02-05CH11231. We are grateful to Dr. David Barton, Dr. Pete Nickias, and Dr. Trevor Ewers from Dow Chemical Co. for fruitful discussions. Joyce R. Araujo and B.S. Archanjo acknowledge CNPq for their fellowships 234217/2014-6 and 234217/2014-6, respectively.

References

1. Sattler JJHB, Ruiz-Martinez J, Santillan-Jimenez E, Weckhuysen BM (2014) Chem Rev 114:10613–10653
2. McFarland E (2012) Science 338:340–342
3. Kumar MS, Chen D, Holmen A, Walmsley JC (2009) Catal Today 142:17–23
4. Chaar MA, Patel D, Kung HH (1988) J Catal 109:463–467
5. Larsson M, Hulten M, Blekkan EA, Andersson B (1996) J Catal 164:44–53
6. Gascon J, Tellez C, Herguido J, Menendez M (2003) Appl Catal A 248:105–116
7. Pham HN, Sattler JJHB, Weckhuysen BM, Datye AK (2016) ACS Catal 6:2257–2264
8. Liu G, Zeng L, Zhao ZJ, Tian H, Wu TF, Gong JL (2016) ACS Catal 6:2158–2162
9. Weckhuysen BM, Bensalem A, Schoonheydt RA (1998) J Chem Soc Faraday Trans 94:2011–2014
10. Sattler JJHB, Gonzalez-Jimenez ID, Luo L, Stears BA, Malek A, Barton DG, Kilos BA, Kaminsky MP, Verhoeven TWGM, Koers EJ et al (2014) Angew Chem Int Ed 53:9251–9256
11. Zheng B, Hua WM, Yue YH, Gao Z (2005) J Catal 232:143–151
12. Sun YN, Wu YM, Tao L, Shan HH, Wang GW, Li CY (2015) J Mol Catal A 397:120–126
13. Khodakov A, Yang J, Su S, Iglesia E, Bell AT (1998) J Catal 177:343–351
14. Tan S, Kim SJ, Moore JS, Liu YJ, Dixit RS, Pendergast JG, Sholl DS, Nair S, Jones CW (2016) ChemCatChem 8:214–221
15. Otroshchenko T, Sokolov S, Stoyanova M, Kondratenko VA, Rodemerck U, Linke D, Kondratenko EV (2015) Angew Chem Int Ed 54:15880–15883
16. Perez-Reina FJ, Rodriguez-Castellon E, Jimenez-Lopez A (1999) Langmuir 15:8421–8428
17. Chen M, Xu J, Su FZ, Liu YM, Cao Y, He HY, Fan KN (2008) J Catal 256:293–300
18. Halasz J, Konya Z, Fudala A, Kiricsi I (1996) Catal Today 31:293–304
19. Zhao ZJ, Chiu CC, Gong JL (2015) Chem Sci 6:4403–4425
20. Liu G, Zhao ZJ, Wu TF, Zeng L, Gong JL (2016) ACS Catal 6:5207–5214
21. Liu Y, Luo C, Liu HC (2012) Angew Chem Int Ed 51:3249–3253
22. Zheng HD, Ou JZ, Strano MS, Kaner RB, Mitchell A, Kalantar-Zadeh K (2011) Adv Funct Mater 21:2175–2196
23. Manthiram K, Alivisatos AP (2012) J Am Chem Soc 134:3995–3998
24. Deb SK (2008) Sol Energy Mater Sol Cells 92:245–258
25. Song JJ, Huang ZF, Pan L, Zou JJ, Zhang XW, Wang L (2015) ACS Catal 5:6594–6599
26. Li YH, Liu PF, Pan LF, Wang HF, Yang ZZ, Zheng LR; Hu P, Zhao HJ, Gu L, Yang HG (2015) Nat Commun 6
27. Belatel H, Al-Kandari, H, Al-Kharafi F, Garin F, Katrib A (2007) Appl Catal A 318:227–233
28. Barton DG, Soled SL, Meitzner GD, Fuentes GA, Iglesia E (1999) J Catal 181:57–72
29. Yang PD, Zhao DY, Margolese DI, Chmelka BF, Stucky GD (1998) Nature 396:152–155
30. Shi JN, Allara DL (1996) Langmuir 12:5099–5108
31. Weckhuysen BM, Verberckmoes AA, Debaere J, Ooms K, Langhans I, Schoonheydt RA (2000) J Mol Catal A 151:pp 115–131
32. Cavani F, Koutyrev M, Trifiro F, Bartolini A, Ghisletti D, Iezzi R, Santucci A, DelPiero G (1996) J Catal 158:236–250
33. Hakuli A, Harlin ME, Backman LB, Krause AOI (1999) J Catal 184:349–356
34. Derossi S, Ferraris G, Fremiotti S, Garrone E, Ghiotti G, Campa MC, Indovina V (1994) J Catal 148:36–46

35. Logie V, Wehrer P, Katrib A, Maire G (2000) J Catal 189:438–448
36. Katrib A, Logie V, Saurel N, Wehrer P, Hilaire L, Maire G (1997) Surf Sci 377:754–758
37. Hemming F, Wehrer P, Katrib A, Maire G (1997) J Mol Catal A 124:39–56